Journal Pre-proof

Enhancing interfacial properties of carbon fiber reinforced epoxy composites by grafting MXene sheets (Ti_2C)

Ruonan Ding, Yan Sun, Jinwoo Lee, Jae Do Nam, Jonghwan Suhr

PII: S1359-8368(20)33627-1

DOI: https://doi.org/10.1016/j.compositesb.2020.108580

Reference: JCOMB 108580

To appear in: *Composites Part B*

Received Date: 26 September 2020

Revised Date: 24 November 2020

Accepted Date: 15 December 2020

Please cite this article as: Ding R, Sun Y, Lee J, Nam JD, Suhr J, Enhancing interfacial properties of carbon fiber reinforced epoxy composites by grafting MXene sheets (Ti_2C), *Composites Part B* (2021), doi: https://doi.org/10.1016/j.compositesb.2020.108580.

CRediT authorship contribution statement

Ruonan Ding: Investigation, Writing original draft, review & editing. **Yan Sun:** Methodology, Investigation. **Jinwoo Lee:** Investigation, Resources. **Jae Do Nam:** Resources. **Jonghwan Suhr:** Funding acquisition, Project administration, Supervision.

Graphic abstract

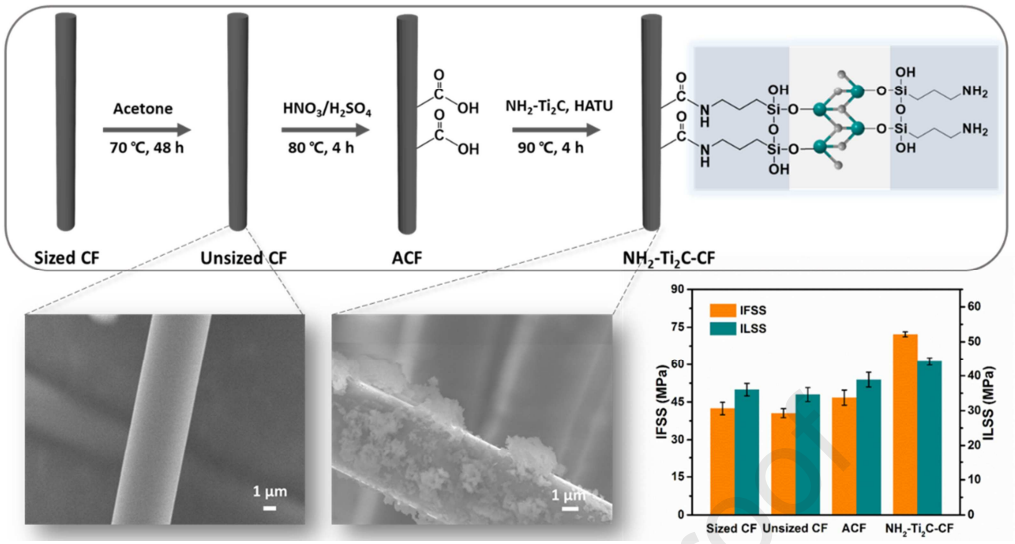

Enhancing interfacial properties of carbon fiber reinforced epoxy composites by grafting MXene sheets (Ti_2C)

Ruonan Ding [a], Yan Sun [a], Jinwoo Lee [b], Jae Do Nam [a,b], Jonghwan Suhr [b,c,*1]

[a] Department of Energy Science, Sungkyunkwan University, 2066, Seoburo, Jangan-gu, Gyeonggi-do, Republic of Korea

[b] Department of Polymer Science & Engineering, Sungkyunkwan University, 2066, Seoburo, Jangan-gu, Gyeonggi-do, Republic of Korea

[c] School of Mechanical Engineering, Sungkyunkwan University, 2066, Seoburo, Jangan-gu, Gyeonggi-do, Republic of Korea

Abstract: MXene (Ti_2C) modified by 3-aminopropyl triethoxysilane was grafted onto carbon fiber (CF) surface in an attempt to improve interfacial properties in continuous CF reinforced epoxy composites. X-ray photoelectron spectroscopy, scanning electron microscopy, and dynamic contact angle test were employed to characterize the effect of the grafted Ti_2C on the interfacial properties. A single fiber fragmentation test together with acoustic emission testing was performed to identify the interface failure mode and also determine the interfacial shear strength (IFSS). The interlaminar shear strength (ILSS) of the laminates was also evaluated with three-point beam testing. It was experimentally observed that Ti_2C sheets were uniformly grafted on the fiber surface with covalent bonding. It could provide not only the increase of the CF surface

* Corresponding author
E-mail: suhr@skku.edu
Tel: 82-31-290-7290

roughness but also an excellent opportunity to create plenty of the polar functional groups thereby leading to a greater surface energy of the CF. The IFSS and ILSS of Ti_2C modified CF composites were enhanced by ~78% and ~28% increase, respectively, compared to ones of unsized CF composites.

Keywords: *Ti_2C, Carbon fiber, Interfacial property, Acoustic emission test*

1. Introduction

Very recently, there has been a surging interest in advanced carbon fiber (CF) composite materials along with their manufacturing. In addition to unmanned air vehicle (UAV) and drone, automotive industries seem to turn their attention to urban air mobility (UAM) and/or personal air vehicle (PAV), which requires lightweight, excellent design flexibility, good corrosion resistance, and outstanding mechanical properties [1-3]. In order to fully exploit the excellent mechanical properties of CF as reinforcement in the composites, there still remains a big challenge which is the enhancement of the interfacial strength between CF and polymer matrix. Typically the interfacial strength is known to be fairly weak due to the poor wettability and interaction caused by hydrophobic and chemically inert CF surface [4]. It is essential to control the interfacial properties in composite design and manufacturing for efficient and effective load transfer from the mechanically weak matrix to the strong CFs under external mechanical stimulus [5]. Consequently, tremendous efforts have been made in the surface grafting of CF to improve the interfacial performance [6-7].

In particular, for decades, nanomaterials including carbon nanotubes [8, 9], nanofibers [10], and graphene oxide (GO) [11, 12] have been widely used as sizing

agents for CF. Various techniques have been explored including electrophoretic deposition, chemical vapor deposition, and chemical grafting [13-15] in order to enhance the interfacial properties hoping to introduce their high mechanical strength, large interface area and high stress transfer capability between the polymer matrix and CF.

Interestingly, Mxene with graphene-like morphology seems to be quite attractive, which is a newly developed 2D nanosheet material synthesized by MAX phases. That is, a ternary carbide or nitride with the general formula $M_{n+1}AXn$; where M, A and X represent early transition metals, group A elements (mainly group III A or group IV A), and carbon or nitrogen. The integer n can be 1, 2 or 3 [16]. The most attractive feature of the MXene will be a number of possible combinations of ensembles of M and X elements by simply etching the A layer from MAX phases, which could provide an ample opportunity to control or engineering the material properties. For instance, it is reported that recent modeling results based on molecular dynamics calculations and density functional theory [17] showed that M_2X MXenes can exhibit much stiffer and stronger mechanical properties than their counterparts of M_3X_2 and M_4X_3. In addition, similar to other carbon based 2D nanosheet material, MXenes can also offer high specific surface area (Ti_2C is 609 m^2/g), hydrophilic surface, and superior mechanical strength (Ti_2C is 0.33±0.07 TPa) over GO (~0.2 TPa) [18-20]. Also, the effective bending rigidity for Ti_2C (D=5.21 eV) greatly exceeds that of graphene (D=2.3 eV) because the monolayer thickness of MXene is about 3 times thicker compare with graphene [21]. Although the cost of MXene is also high as of today, the potential of

MXene with outstanding mechanical properties as well as large surface area could allow for the use of the new material in a wide variety of engineering applications in the near future. Here, this study focuses on the investigation of MXene as an interphase material between CF and the epoxy matrix in order to improve the interfacial strength in the composites. The interest of MXene in this study is selected as Ti_2C. To the best of our knowledge, few articles have reported the use of Ti_2C by chemical grafting for CF composites.

This study demonstrates an efficient approach to modify the composite interphase by grafting Ti_2C with chemical covalent bonding, resulting in the significantly improved adhesion between CF and epoxy matrix. The interfacial shear strength (IFSS) and the interlaminar shear strength (ILSS) of the Ti_2C modified CF composites are measured to be 72.17 MPa, and 44.24 MPa showing the improvement of 77.9 % and 27.8 % respectively over unsized composite counterparts. This study could show the great potential of the use of Ti_2C to effectively engineer the interfacial characteristics of CF composites, and eventually design and manufacture lightweight super strong composite structures with high reliability for various load carrying structures in aircraft, watercraft or ground vehicle.

2. Experimental section

2.1 Materials

Unidirectional carbon fiber (12K Carbon Multifilament Continuous Tow, tensile strength 696–725 KSI) was purchased from Fibre Glast Developments Corporation, USA (**Table S1**). Ti_2AlC (≤400 mesh, 99.5 %) was commercially available from

Famouschem Technology (Shanghai) Co., Ltd. The epoxy resin (YD-128) was supplied by KUKOO chemical Co., Ltd. The other chemicals including diethylenetriamine, nitric acid, (3-Aminopropyl) triethoxysilane (APTES), sulfuric acid, hydrofluoric acid, 2-(7-Azabenzotriazol-1-yl)-N,N,N',N'-tetramethyluronium hexafluorophosphate (HATU), acetone, dimethyl sulfoxide, and N,N-dimethylformamide (DMF)were purchased from Sigma-Aldrich.

2.2 CF surface grafting process

Firstly, the Ti_2C sheets were functionalized by utilizing APTES after synthesis from Ti_2AlC (**Fig. S1,2**), which was referred as NH_2-Ti_2C. The schematic of the chemical reaction is illustrated in **Fig. 1a**. Then the commercially available CF called 'sized CF' was refluxed with acetone solution at 70 □ for 48 h to remove the sizing agent. It is referred as 'unsized CF'. The unsized CF was oxidized in HNO_3 and H_2SO_4 (1:3) mixture at 80 °C for 4 h. The resultant carbon fibers were referred as 'ACF'. The ACF was placed into the well-mixed solution of 6 mg NH_2-Ti_2C, 5 mg HATU, and 30 ml DMF. The chemical reaction for a grafting process was carried out at 90 □ for 4 h to eventually obtain NH_2-Ti_2C-CF. During the grafting process, the reaction between the carboxyl groups of ACF and amino groups of NH_2-Ti_2C was completed with the aid of HATU as a condensing agent. The schematic of the overall chemical process and reaction is shown in **Fig. 1b**.

2.3 Preparation of specimens for IFSS and ILSS test

For the IFSS test, single fiber fragmentation specimens were prepared according to the ASTM D638 standard (**Fig. S3**). Short beam strength test was employed to analysis

ILSS. The composite laminate specimens were fabricated using the hand layup method shown in supporting information. The repeat number of each tests was 10.

2.4 Characterization

The chemical components grafted on the CF surface were analyzed by XPS (K-Alpha, Thermo Fisher Scientific Inc., USA). The surface morphology of CF and the interfacial failure were examined with SEM (JSM-7500F, JEOL, USA). The contact angle between the CF and the test liquids was measured using a dynamic contact angle meter (DCAT21, Data Physics Instruments, Germany). The detailed description was shown in supporting material (**Fig. S4**). Deionized water (γ^d= 21.8 mJ/m^2, γ= 72.8 mJ/m^2) and diiodomethane (γ^d= 50.8 mJ/m^2, γ= 50.8 mJ/m^2, 99 % purity, Alfa Aesar, USA) were used as test liquids [22]. The dispersive and polar components can be calculated by the following equations:

$$\gamma_l(1+cos\theta) = 2\sqrt{\gamma_l^p\gamma_f^p} + 2\sqrt{\gamma_l^d\gamma_f^d} \quad (1)$$

where, γ_l , γ_l^p , and γ_l^d are the surface tension, polar component, and dispersive components, respectively.

The single fiber tensile test was carried out with the Instron 3343 universal testing machine. The dimension of the specimen is shown in **Fig. S3b**. A total of 50 samples were tested. The fiber fragmentation was monitored and observed through a metallographic microscope (OLYMPUS BX51, Guangzhou).

For the single fiber fragmentation test, the specimen was subjected to a uniaxial tensile load at a crosshead speed of 2 mm/min using the Instron E3000 Universal testing machine. The IFSS was determined with the Kelly–Tyson equation [23].

$$\tau_{\text{IFSS}} = \frac{\sigma_f}{2}\frac{d}{l_c} \quad (2)$$

where, d is the fiber diameter, σ_f is the fiber strength at the critical fragmentation length (l_c), which can be obtained from the average fiber fragment length ($\bar{l}$) at saturation.

$$l_c = \frac{4}{3}\bar{l} \quad (3)$$

Since the direct measurement of the fiber strength at the critical fragment length presents very challenging, σ_f can be often determined using the following empirical formula using a single fiber tensile strength test.

$$\sigma_f = \sigma_0\left(\frac{l_0}{l_c}\right)^{1/\beta} \quad (4)$$

where, l_0 is the initial length of the single carbon fiber, σ_0 is the fiber tensile stress, and β is the Weibull shape parameter obtained through the linear fitting.

During the single fiber fragmentation test, the acoustic emission (AE) test was concurrently performed to evaluate the fracture process between CF and epoxy resin. The AE signals were acquired by a wideband AE sensor (Physical Acoustic Corp., (PAC)).

The beam shear testing was conducted to characterize the ILSS of the unidirectional CF composite laminates according to ASTM D2344 (**Table S2**). The measured samples with the dimensions of 12.48 mm × 4.16 mm × 2.08 mm. The characterization was performed in a universal testing machine (DTU-M series, Dae Kyung Tech, KR) at a crosshead speed of 1 mm/min. The ILSS was determined using the following formula:

$$ILSS = \frac{0.75P}{bh} \quad (5)$$

where, P is the maximum load observed during the test, and b and h are the width and

thickness of the specimen, respectively.

3. Results and discussion

3.1 Chemical composition and morphology of CF surface

The surface chemical compositions of Ti_2C before and after APTES modification were investigated with XPS. As shown in **Fig. 2b**, the O 1s peaks of Ti_2C are resolved into two component peaks identified as Ti-O (530.4 eV) and C−O (532.3 eV), respectively. After the addition of APTES, the new peak of Si-O-Ti (533.3 eV) is detected in the O 1s spectra of NH_2-Ti_2C (**Fig. 2c**). The presence of the Si-O-Ti bond can be a good indication of successfully grafting APTES onto Ti_2C via covalent bonds.

The unsized CF surface is found to consist of mainly carbon and oxygen (C = 87.93 %, O = 12.07 %) (**Fig. 2a**) with C-C (284.7 eV), C-O (285.4 eV), and C = O (289.9 eV) bonds. After acid treatment, the concentration of carbon moderately decreases while one of the oxygen considerably increases up to 19.81 %, probably thanks to the generation of –COOH group onto CF. Newly generated elements, including F, Ti, and Si are found to appear while the content of N increases after grafting NH_2-Ti_2C onto CF, which can clearly confirm the existence of NH_2-Ti_2C. Furthermore, a new C 1s peak at 287.9 eV is also found in **Fig. 2f**, which may be attributed to the newly created bond (-N-C=O). The bond is formed by the carboxyl group of ACF and the amino group of NH_2-Ti_2C. This chemical bond can also be confirmed in the N 1s spectrum (**Fig. 2g**), where an amide (-N-C=O) peak appears at 400.1 eV [24]. These results (**Fig. S5, 6**) indicate that NH_2-Ti_2C seems to very likely interact with ACF through covalent bonds, ensuring a chemical grafting.

The remarkable change in the surface morphology of CF after the NH_2-Ti_2C surface modification was observed through SEM characterization (**Fig. 3**). After the removal of as-received sizing, a smooth CF surface is observed with a slightly reduced diameter (**Fig. 3b**). However, some narrow shallow and parallel grooves are seen on the fiber surface after acid treatment (**Fig. 3c**), which is likely attributed to acid oxidation and etching. Once grafting with NH_2-Ti_2C, the newly sized CF surface is found to have numerous NH_2-Ti_2C sheets as shown in **Figs. 3d,e** compared to the smooth surface of the unsized CF. The SEM characterization can indicate that the NH_2-Ti_2C sheets are covalently grafted and abundantly distributed onto the fiber surface along the length. It can indicate that they could offer an ample opportunity for efficient and effective control of interfacial characteristics between the CF and matrix with much larger interfacial area and also provide a chance to strengthen the interface with mechanical interlocking between them.

3.2 The surface energy of CF

The surface energy of each CF during the grafting process was investigated by measuring the contact angle using two different liquids: deionized water and diiodomethane (**Fig. 3f**). As shown in **Fig. 3g**, the surface energy increases from 33.9 mJ/m^2 for sized CF to 38.8 mJ/m^2 for unsized CF. After acid oxidation, the surface energy of ACF goes up to 56.0 mJ/m^2. Meanwhile, the increase of both polar and dispersive components were observed. Moreover, with the grafting of NH_2-Ti_2C sheets, NH_2-Ti_2C-CF shows a higher polar component of 20.1 mJ/m^2 and a dispersive component of 46.6 mJ/m^2. Consequently, the total surface energy increased up to 66.7

mJ/m^2. It is reported that more polar groups arising from the grafted NH_2-Ti_2C can contribute to the increase in the polar component, while the greater roughness can give rise to the higher dispersive component resulting from NH_2-Ti_2C participation [25]. It can be expected that the enhanced hydrophilicity and wettability of the NH_2-Ti_2C-CF would improve the interfacial strength between the fiber and polymer matrix in composites (**Table S3**).

3.3 Evaluation of Interfacial properties

The effect of NH_2-Ti_2C sheets on the interfacial strength was examined by characterizing IFSS and ILSS. As shown in **Table 1**, the removal of commercially as-received fiber sizing decreases IFSS from 42.38 to 40.57 MPa. After oxidation, the IFSS is slightly increased up to 46.73 MPa, owing to the generation of -COOH groups on the CF surface, which can react with hydroxyl and oxirane groups of epoxy resin to form a chemical bond. Noticeably, the IFSS increases from 40.57 to 72.17 MPa after grafting NH_2-Ti_2C sheets, improved by 77.9 % while the tensile strength is slightly decreased by only 3.8% in comparison with that of unsized CF. Very similar to IFSS evaluation of the composites, NH_2-Ti_2C-CF laminate has the highest ILSS value (44.24 MPa), enhanced by 27.8 % compared with that of unsized CF laminate (34.63 MPa). Obviously, the observed improvement of the interfacial properties is believed to be attributed to the existence of NH_2-Ti_2C. It seems that the grafting of NH_2-Ti_2C onto CF not only creates a strong chemical covalent bond between them (**Figs. 2f, g**) but also introduces both mechanical and chemical interlocking between CF and epoxy resin since epoxy monomers inter-diffuse through NH_2-Ti_2C sheets and chemically interact

with the amine groups of the NH_2-Ti_2C. Thus, it could imply that the correspondingly greater strength may be required to pull the NH_2-Ti_2C out of the resin. (**Fig. S7**). The IFSS results are also compared to the relevant literature values associated with similar grafting methods. The literature survey indicates that Ti_2C can outperform the interfacial characteristics in the composites compared to other nanomaterials reported so far (**Table S4**).

Additionally, for the unsized CF, the average length of fragmentation is found to be about 592.6 μm, while after grafting NH_2-Ti_2C-CF on its surface, the corresponding length is measured to be only about 386.5 μm (**Table 1**). The observed shorter fragmentation length of NH_2-Ti_2C-CF results from the combination of higher IFSS and the lower fiber strength. The formation of smaller fragments in NH_2-Ti_2C-CF composite can also be found in birefringence pattern shown in **Fig. 4**. The NH_2-Ti_2C-CF composite exhibits the more concentrated and smaller birefringent pattern as seen in **Fig. 4b**, which must be associated with strong adhesion. For the unsized CF composite, there are large break gaps and obvious debonded interfaces (**Fig. 4a**). This could result from relatively weak interface bonding strength and stress transfer efficiency [26]. Therefore, a full debonding phenomenon often occurs at the interface as shown in **Fig. 4c**. In contrast, it was found that the interaction between NH_2-Ti_2C-CF and the epoxy matrix was stronger, and there was no obvious debonding or pulling out (**Fig. 4d**). Similar phenomena can also be found in NH_2-Ti_2C-CF laminate shown in **Fig. S8**.

3.4 Failure mechanisms in CF composites

To investigate the mechanisms responsible for the failures observed in the CF

reinforced polymer composites, the AE testing was also conducted along with the SFFT (**Fig. S9**) [27-30]. The AE signals for every event monitored during the tensile testing were analyzed to identify the peak frequency. It is reported that the peak frequency can be characterized to identify failure modes in continuously reinforced fiber composites [31,32]. As seen in **Figs. 5a and b**, three distinct peak frequency ranges of both unsized CF and NH_2-Ti_2C-CF composites are clearly found, displaying three failure modes: matrix cracking (50–120 kHz), interface failure (120–300 kHz), and fiber breakage (>300 kHz) [33]. **Figs. 5c and d** compare the accumulative number of the AE events corresponding for the three failure modes of the composites, respectively. These results can provide us with three important observations. When compared to the unsized composites, first far more fiber breaks are generated in NH_2-Ti_2C-CF composites, and secondly, more matrix cracks are found in NH_2-Ti_2C-CF composites. Lastly, the fraction of the interface failures from the total number of failures however seems to be much lower in NH_2-Ti_2C-CF composites and also, importantly, the 'Interface onset' occurs almost simultaneously with the 'Fiber onset' (**Fig. 5d)**, while the 'Interface onset' comes first and the 'Fiber onset' appears later in unsized CF composite (**Fig. 5c**). Note that both 'Fiber onset's in two composites appear at the almost same strain.

It is reported that the fiber/matrix interface debonding is caused by fiber breaks in the composite [34]. However, at the interface of NH_2-Ti_2C-CF composites, NH_2-Ti_2C sheets are found to play a bridge role to strongly link between fiber and matrix through a chemical bond (**Fig. 6c**)**.** This can allow for the NH_2-Ti_2C sheets to transfer much more stress into the matrix and prevent the crack propagation along the interface when the

single fiber is broken into a number of short fibers. As a consequence, although the numerous fiber breaks are generated, less interface failures are found and a lot of microcracks within the matrix are developed, as illustrated in **Fig. 6b**. In fact, the SEM characterization of the fracture surface morphology (**Figs. 4c, d** and **Fig. S10**) can confirm the aforementioned observations. It was examined that the partial interface debonding between fiber and matrix in the NH_2-Ti_2C-CF composites is often observed, while the fiber pull-out and full debonding are found in the unsized composites.

4. Conclusion

In this study, MXene (Ti_2C), which is a newly developed 2D material, was investigated to enhance the interfacial strength between CF and epoxy resin. The chemically modified Ti_2C (NH_2-Ti_2C) was successfully grafted onto CF through covalent bonds (-C=O-NH-). The SEM characterization and contact angle measurements indicated that the grafting of NH_2-Ti_2C not only increased the roughness of CF surface but also introduced plenty of polar functional groups thereby leading to much greater surface energy of CF. It was experimentally observed that the IFSS and ILSS of NH_2-Ti_2C-CF composite were significantly enhanced by 77.9 % and 27.8 % increase, respectively, when compared with those of the unsized CF composites. These enhancements were also confirmed with the analysis and examination of birefringence pattern and fracture morphology of the composites. Furthermore, the failure modes of the composites were identified by interpreting the AE signals which were concurrently being monitored during the SFFT. It showed that less interface failures and more matrix microcracks were developed in NH_2-Ti_2C-CF composites, indicating the strong

interface adhesion and better load transfer capability between the fiber and matrix. This study can show that, if optimized, the interfacial strength of CF reinforced composites could be dramatically enhanced, and effectively and efficiently controlled so that the excellent mechanical properties of CF can be fully exploited for a wide variety of composite structures.

Acknowledgment

This work was supported by the National Research Foundation of Korea (NRF) grant funded by the Korea government (MSIP) [No. 2018R1A2B2001565]

References

[1] Lapeña-Rey N, Blanco J, Ferreyra E, Lemus J, Pereira S, Serrot E. A fuel cell powered unmanned aerial vehicle for low altitude surveillance missions. International Journal of Hydrogen Energy. 2017;42(10):6926-40.

[2] Courtin C, Burton MJ, Yu A, Butler P, Vascik PD, Hansman RJ. Feasibility study of short takeoff and landing urban air mobility vehicles using geometric programming. 2018 Aviation Technology, Integration, and Operations Conference2018. p. 4151.

[3] Zdunich P, Bilyk D, MacMaster M, Loewen D, DeLaurier J, Kornbluh R, et al. Development and testing of the mentor flapping-wing micro air vehicle. Journal of Aircraft. 2007;44(5):1701-11.

[4] Xu H, Zhang X, Liu D, Yan C, Chen X, Hui D, et al. Cyclomatrix-type polyphosphazene coating: Improving interfacial property of carbon fiber/epoxy composites and preserving fiber tensile strength. Composites Part B: Engineering. 2016;93:244-51.

[5] Gao S-L, Mäder E, Zhandarov SF. Carbon fibers and composites with epoxy resins: Topography, fractography and interphases. Carbon. 2004;42(3):515-29.

[6] Yao X, Gao X, Jiang J, Xu C, Deng C, Wang J. Comparison of carbon nanotubes and graphene oxide coated carbon fiber for improving the interfacial properties of carbon fiber/epoxy composites. Composites Part B: Engineering. 2018;132:170-7.

[7] Gao B, Zhang R, He M, Wang C, Liu L, Zhao L, et al. Interfacial microstructure and mechanical

properties of carbon fiber composites by fiber surface modification with poly (amidoamine)/polyhedral oligomeric silsesquioxane. Composites Part A: Applied Science and Manufacturing. 2016;90:653-61.

[8] Zhao M, Meng L, Ma L, Ma L, Yang X, Huang Y, et al. Layer-by-layer grafting CNTs onto carbon fibers surface for enhancing the interfacial properties of epoxy resin composites. Composites Science and Technology. 2018;154:28-36.

[9] Gonzalez-Chi P, Rodríguez-Uicab O, Martin-Barrera C, Uribe-Calderon J, Canché-Escamilla G, Yazdani-Pedram M, et al. Influence of aramid fiber treatment and carbon nanotubes on the interfacial strength of polypropylene hierarchical composites. Composites Part B: Engineering. 2017;122:16-22.

[10] Lee JU, Park B, Kim B-S, Bae D-R, Lee W. Electrophoretic deposition of aramid nanofibers on carbon fibers for highly enhanced interfacial adhesion at low content. Composites Part A: Applied Science and Manufacturing. 2016;84:482-9.

[11] Kwon YJ, Kim Y, Jeon H, Cho S, Lee W, Lee JU. Graphene/carbon nanotube hybrid as a multi-functional interfacial reinforcement for carbon fiber-reinforced composites. Composites Part B: Engineering. 2017;122:23-30.

[12] Jang H-K, Kim H-I, Dodge T, Sun P, Zhu H, Nam J-D, et al. Interfacial shear strength of reduced graphene oxide polymer composites. Carbon. 2014;77:390-7.

[13] Zheng Y, Chen L, Wang X, Wu G. Modification of renewable cardanol onto carbon fiber for the improved interfacial properties of advanced polymer composites. Polymers. 2020;12(1):45.

[14] Kinloch IA, Suhr J, Lou J, Young RJ, Ajayan PM. Composites with carbon nanotubes and graphene: An outlook. Science. 2018;362(6414):547-53.

[15] Zheng Y, Wang X, Wu G. Chemical modification of carbon fiber with diethylenetriaminepentaacetic acid/halloysite nanotube as a multifunctional interfacial reinforcement for silicone resin composites. Polymers for Advanced Technologies. 2020;31(3):527-35.

[16] Xie Y, Naguib M, Mochalin VN, Barsoum MW, Gogotsi Y, Yu X, et al. Role of surface structure on Li-ion energy storage capacity of two-dimensional transition-metal carbides. Journal of the American Chemical Society. 2014;136(17):6385-94.

[17] Tang Q, Zhou Z, Shen P. Are MXenes promising anode materials for Li ion batteries? Computational studies on electronic properties and Li storage capability of Ti_3C_2 and $Ti_3C_2X_2$ (X= F,

OH) monolayer. Journal of the American Chemical Society. 2012;134(40):16909-16.

[18] Zhang H, Liang G, Gu A, Yuan L. Facile preparation of hyperbranched polysiloxane-grafted aramid fibers with simultaneously improved UV resistance, surface activity, and thermal and mechanical properties. Industrial & Engineering Chemistry Research. 2014;53(7):2684-96.

[19] Borysiuk VN, Mochalin VN, Gogotsi Y. Molecular dynamic study of the mechanical properties of two-dimensional titanium carbides $Ti_{n+1}C_n$ (MXenes). Nanotechnology. 2015;26(26):265705.

[20] Naguib M, Mashtalir O, Carle J, Presser V, Lu J, Hultman L, et al. Two-dimensional transition metal carbides. ACS nano. 2012;6(2):1322-31.

[21] Borysiuk VN, Mochalin VN, Gogotsi Y. Bending rigidity of two-dimensional titanium carbide (MXene) nanoribbons: A molecular dynamics study. Computational Materials Science. 2018;143:418-24.

[22] Wang C, Li J, Sun S, Li X, Zhao F, Jiang B, et al. Electrophoretic deposition of graphene oxide on continuous carbon fibers for reinforcement of both tensile and interfacial strength. Composites Science and Technology. 2016;135:46-53.

[23] Kelly A, Tyson aW. Tensile properties of fibre-reinforced metals: copper/tungsten and copper/molybdenum. Journal of the Mechanics and Physics of Solids. 1965;13(6):329-50.

[24] Wang C, Li J, Yu J, Sun S, Li X, Xie F, et al. Grafting of size-controlled graphene oxide sheets onto carbon fiber for reinforcement of carbon fiber/epoxy composite interfacial strength. Composites Part A: Applied Science and Manufacturing. 2017;101:511-20.

[25] Zhang R, Gao B, Ma Q, Zhang J, Cui H, Liu L. Directly grafting graphene oxide onto carbon fiber and the effect on the mechanical properties of carbon fiber composites. Materials & Design. 2016;93:364-9.

[26] Zhang B, Sun X, Liu C, Zhao S. Study on the monofilament fracture damage pattern and stress field in fracture experiment. Journal of Reinforced Plastics and Composites. 2012;31(20):1377-87.

[27] Bourchak M, Farrow I, Bond I, Rowland C, Menan F. Acoustic emission energy as a fatigue damage parameter for CFRP composites. International Journal of Fatigue. 2007;29(3):457-70.

[28] Gutkin R, Green C, Vangrattanachai S, Pinho S, Robinson P, Curtis P. On acoustic emission for failure investigation in CFRP: Pattern recognition and peak frequency analyses. Mechanical systems and signal processing. 2011;25(4):1393-407.

[29] Pashmforoush F, Fotouhi M, Ahmadi M. Damage characterization of glass/epoxy composite under three-point bending test using acoustic emission technique. Journal of materials engineering and performance. 2012;21(7):1380-90.

[30] Ni Q-Q, Iwamoto M. Wavelet transform of acoustic emission signals in failure of model composites. Engineering Fracture Mechanics. 2002;69(6):717-28.

[31] Jiang W, Zhang Q, Zhang Y, Guo Z, Tu S-T. Flexural behavior and damage evolution of pultruded fibre-reinforced composite by acoustic emission test and a new progressive damage model. International Journal of Mechanical Sciences. 2020;188:105955.

[32] Brunner AJ. Fiber-reinforced polymer composites test specimen design for selected damage mechanisms. Proceedings of the Institution of Mechanical Engineers, Part L: Journal of Materials: Design and Applications. 2019;233(3):328-37.

[33] Suzuki M, Nakanishi H, Iwamoto M, Jinen E. Application of static fracture mechanisms to fatigue fracture behavior of class A-SMC composite. Japan-U S Conference on Composite Materials, 4 th, Washington, DC1989. p. 297-306.

[34] Zhao F, Takeda N. Effect of interfacial adhesion and statistical fiber strength on tensile strength of unidirectional glass fiber/epoxy composites. Part I: experiment results. Composites Part A: Applied Science and Manufacturing. 2000;31(11):1203-14.

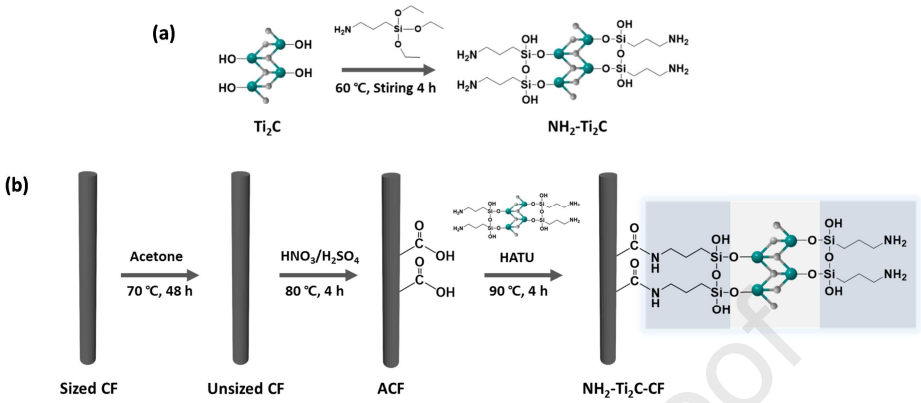

Fig. 1. (a) Schematic illustration of Ti_2C modification and (b) grafting of NH_2-Ti_2C on the CF surface.

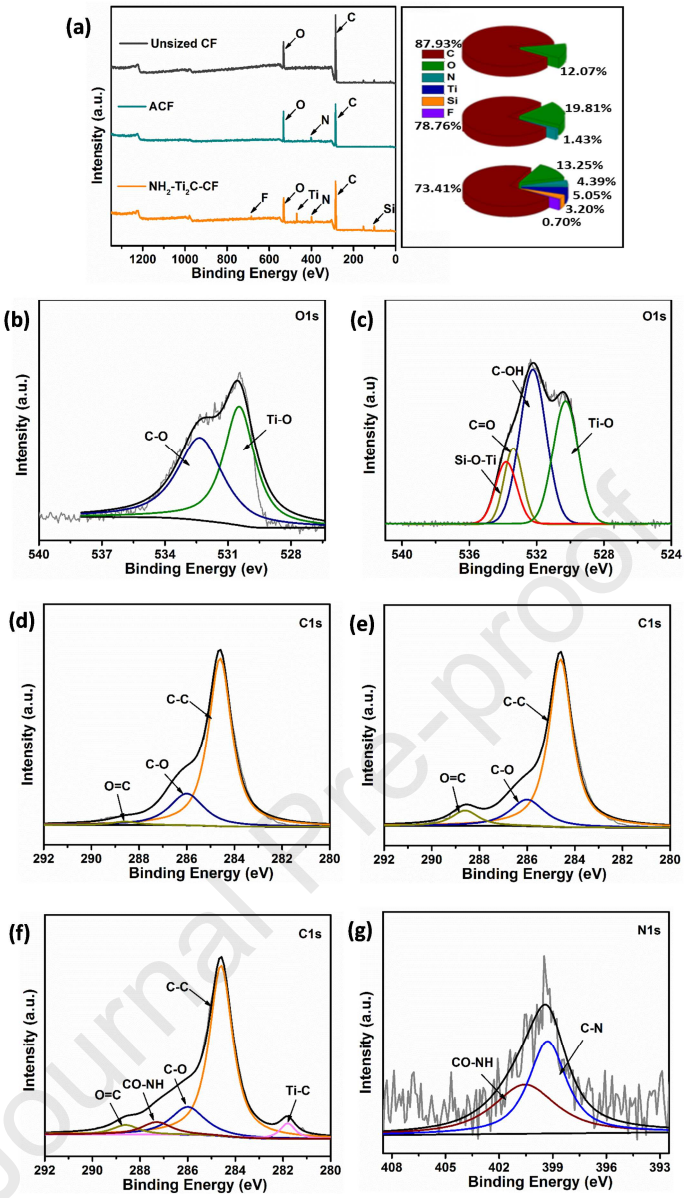

Fig. 2. (a) Wide scan XPS spectra. O 1s high resolution XPS spectra of (b) Ti_2C, and (c) NH_2-Ti_2C. C 1s high resolution XPS spectra of (d) unsized CF, (e) ACF, (f) NH_2-Ti_2C-CF, (g) N 1s high resolution XPS spectra of NH_2-Ti_2C-CF.

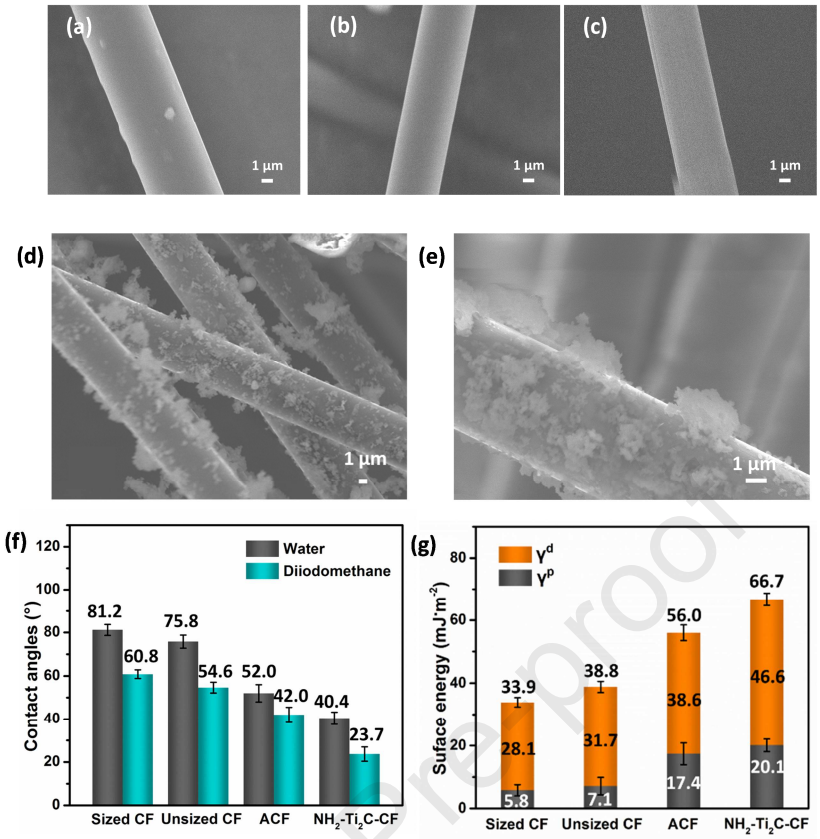

Fig. 3. Morphologies of CF: (a) sized CF, (b) unsized CF, (c) ACF, (d) NH_2-Ti_2C-CF, and (e) its high resolution. (f) Contact angle and, (g) surface energy of various carbon fibers.

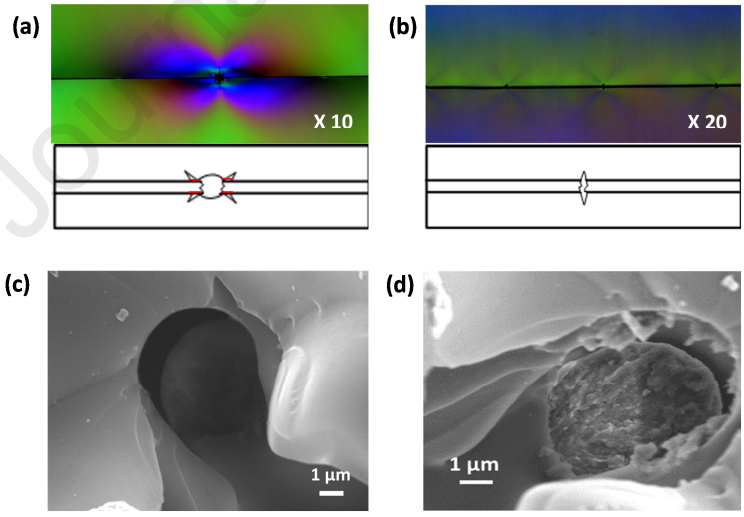

Fig. 4. Birefringence pattern of single fiber fragmentation tests (a) unsized CF composite, (b) NH_2-Ti_2C-CF composite. Cross-section fracture morphology of single fiber fragmentation tests (c) unsized CF composite, (d) NH_2-Ti_2C-CF composite.

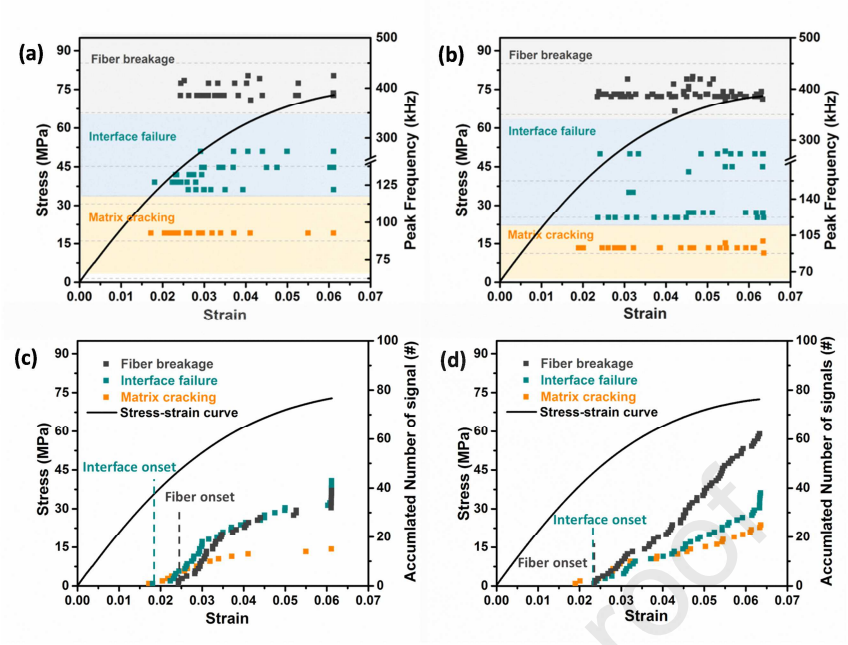

Fig. 5. Event peak frequency versus strain for (a) unsized CF composite and (b) NH_2-Ti_2C-CF composites during single fiber fragmentation test. The number of signals accumulated by different events versus strain for (c) unsized CF composite and (d) NH_2-Ti_2C-CF composite.

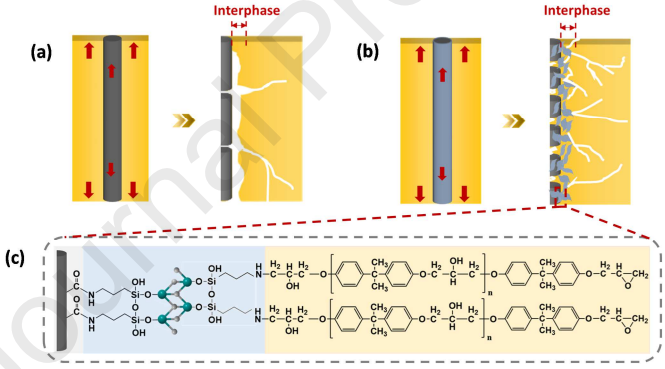

Fig. 6. Schematic illustration of three failures (fiber breakage, interface failure and matrix cracking) of single fiber composite reinforced with (a) unsized CF, (b) NH_2-Ti_2C-CF. (c) The chemical reaction of NH_2-Ti_2C between ACF and epoxy.

Table 1. SFFT and ILSS results for each type of carbon fiber.

CF Types	Critical Length l_c (μm)	Gauge Length l_0 (mm)	Fiber Strength $\sigma_{f,l0}$ (GPa)	W. shape β	Diameter d (μm)	Fiber Critical Strength $\sigma_{f,lc}$ (GPa)	IFSS τ (MPa)	ILSS (MPa)
Sized CF	587.7	5.134±0.11	4.86±0.45	4.01	5.93±0.03	8.3441	42.38±2.5	36.01±1.8
Unsized CF	592.6	5.128±0.20	4.77±0.51	3.66	5.59±0.09	8.6016	40.57±1.8	34.63±2.0
ACF	539.5	5.198±0.15	4.53±0.34	3.28	5.58±0.08	9.0375	46.73±3.0	38.92±2.1
NH_2-Ti_2C-CF	386.5	5.213±0.13	4.59±0.55	3.30	5.97±0.71	9.3445	72.17±1.0	44.24±1.1

Declaration of competing interest

The authors declare that they have no known competing financial interests or personal relationships that could have appeared to influence the work reported in this paper.